

A LABORATORY STUDY INVESTIGATING OZONE EFFECTS ON TRANSPIRATION, CARBON ASSIMILATION, AND PHOTOSYNTHESIS BY PERTURBING STOMATAL DIFFUSIVE RESISTANCE

Jacob Bushey¹, Madeline Miles¹, Laura Barry¹, Manuel Lerdau¹, Xi Yang¹, Gabriel Isaacman-VanWertz² and Sally Pusede¹

¹University of Virginia, Environmental Sciences, Charlottesville, VA, United States

²Virginia Polytechnic Institute and State University, Civil and Environmental Engineering, Blacksburg, VA, United States

Abstract

Tropospheric ozone (O₃) is an air pollutant that is harmful to plants and ecosystems, with plants primarily exposed through stomatal uptake. O₃ stomatal uptake has been shown to reduce carbon assimilation through direct impacts on photosynthesis and by disrupting stomatal control; however, relationships between these two effects are not well understood. Here, we describe a series of laboratory experiments in which we manipulate stomatal diffusive resistance by conducting experiments in both air (80% N₂, 20% O₂) and its analog He/O₂ (80% He, 20% O₂) under both low and high O₃ conditions. The approach allows us to alter stomatal conductance without affecting other aspects of leaf metabolism and the within-chamber O₃ lifetime. Experiments use ozone-exposed sweetgum trees, *Liquidambar styraciflua*, continuously monitoring O₃ and CO₂ uptake, transpiration, leaf temperature, and chlorophyll fluorescence, a proxy for photosynthetic electron transport. Our methodology allows us to observe the dynamics of O₃ uptake, which we find to be stomatally limited, with no evidence for an additional internal rate-limiting resistance. We show that isolated elevated O₃ exposures do not affect transpiration, carbon assimilation, or their coupling.

Introduction

Tropospheric ozone is an air pollutant that is harmful to plants, ecosystems, and human health. It forms via photochemical reactions between nitrogen oxides (NO_x) and biogenic volatile organic compounds (BVOCs). Plants are primarily exposed to O₃ via uptake through their stomata. Studies have shown that O₃ stomatal uptake reduces carbon assimilation in plants, due to both direct impacts on photosynthesis and a disruption of stomatal control. The relationship between these two effects is not well understood, however, and different studies place contradictory emphasis on which is the primary driver of O₃ damage to the plant. Past studies have attempted to clarify this ambiguity by manipulating stomatal aperture, exposing the plant to controlled O₃ treatment levels, and monitoring the plant's response. Using various stimuli, such as varying levels of photosynthetically active

radiation (PAR), varying levels of drought stress, and treatment with abscisic acid, the experiments are able to manipulate stomatal aperture. Unfortunately, each of these methods influences another part of the plant's metabolism, which introduces confounding variables to these studies. In order to determine the mechanism of O₃ damage to the plant, it is necessary to vary stomatal conductance independently. The goal of this experiment was to implement a procedure that would allow the stomatal aperture to be manipulated without altering another part of the plant's metabolism, enabling us to determine the mechanism by which O₃ exposure reduces carbon assimilation.

Such a methodology was used by Parkhurst & Mott in 1990 to study intercellular diffusion, and again in 1991 to study stomatal responses to humidity. By conducting experiments in both air (80% N₂, 20% O₂) and its analog

HelOx (80% He, 20% O₂), they were able to directly manipulate stomatal diffusive resistance, without introducing confounding variables. Because the diffusive resistance of HelOx is so much lower than air, such that diffusion across the stomata occurs 2.33 times more rapidly in an atmosphere of HelOx than air (Mott & Parkhurst 1991), the stomata contract to reduce water loss. We adopted the same principles to test stomatal responses to tropospheric O₃.

We investigated two other phenomena reported in the literature — stomatal sluggishness and decoupling. Stomatal sluggishness, a delay in the ability of the stomata to dilate and contract in the response to changing stimuli because of hysteresis in stomatal aperture, has previously been observed under conditions of elevated O₃ (Torsethaugen et al., 1999; Paoletti & Grulke, 2010). Decoupling of photosynthesis and stomatal conductance of carbon dioxide across the stomata have been observed in response to elevated O₃ (Lombardozzi et al., 2012).

Using an experimental setup similar to Delaria et al. (2018), we were able to test individual leaves clipped from an American sweetgum tree (*Liquidambar styraciflua*) under both low (15 ppb) and high (75 ppb) O₃ conditions. Continuous monitoring of O₃ and CO₂ uptake, transpiration, and chlorophyll fluorescence allow us to evaluate the plant's response to various levels of ozone exposure. Chlorophyll fluorescence is quantified using pulse-amplitude modulation (PAM) fluorometry is used to monitor leaf fluorescence (SIF), a proxy for the electron transport rate in photosynthesis.

Measurements and Methods

American Sweetgum Cuttings. Branch cuttings were obtained from a stand of established American sweetgum trees (*Liquidambar styraciflua*) on the main grounds of the University of Virginia in Charlottesville, Virginia. Experiments were conducted in

June – August 2021, during which time local mean daytime (6 am – 8 pm local time, LT) atmospheric O₃ mixing ratios were 35.16 ppb, nighttime (8 pm – 6 am LT) O₃ mixing ratios were 20.38 ppb, and the 3-month W126 value was 4 ppm h for the ozone monitoring season of April 1, 2021 – September 30, 2021, according to measurements collected at the nearby Virginia Department of Environmental Quality monitoring station (38.077, -78.504). Branch cuttings were collected each morning, brought promptly to the laboratory, submerged in water, and re-cut at a diagonal below the water line. One leaf on the cutting was situated in the chamber and dark adapted in an air atmosphere under experimental CO₂, humidity, and temperature conditions. After each experiment, the leaf was pressed, stored, photographed, and its area measured using ImageJ, a Java-based image processing program.

Gas Exchange Measurements. We conducted our experiments using a custom flow-through chamber consisting of a suspended Teflon bag (10 in \times 10 in \times 6 in; Ingeniven Fluoropolymers). An opening sleeve on one chamber face allowed isolation of individual leaves by loosely cinching the sleeve around the leaf petiole. A PTFE-coated fan was placed inside the chamber to cause turbulent mixing and minimize leaf boundary layer resistance and leading to a slight but visible leaf flutter (Meixner et al., 1997; Pape et al., 2009; Breuninger et al., 2013). An overhead lamp provided photosynthetically active radiation (PAR) of approximately 850 $\mu\text{mol m}^{-2} \text{s}^{-1}$ at the leaf surface, which was below the light saturation threshold so as to not induce oxidation effects that potentially confound the effects of O₃ uptake. We monitored the PAR flux density continuously outside of the chamber for the duration of each experiment (LI-190R Quantum Sensor).

The chamber atmosphere was alternated between “air” (79:21 v/v N₂/O₂) and its helium analog “HelOx” (87% 79:21 v/v He/O₂; 13%

79:21 v/v N₂/O₂). The total chamber inflow was 4.6 L min⁻¹, with 4 L min⁻¹ of commercial dry air and HelOx mixtures (Praxair AI0.0UZ or HEOX20C) and 1.9 mL min⁻¹ of a pure (99.9%) CO₂ gas standard (Praxair, CD 3.0). For both the air and HelOx conditions, 0.3 L min⁻¹ of air saturated with water vapor (H₂O_(v)) and 0.3 L min⁻¹ of O₃ enriched air were added to the bulk flow. In both cases, the air stream was saturated using a bubbler equipped with a glass frit, and a droplet trap was placed in-line to prevent the addition of large droplets to the bulk flow. O₃ was produced with a Thermo Fisher Scientific Model 146iQ ozone generator supplied with dry zero air (Praxair AI0.0UZ). Gas flow was controlled using Alicat mass flow controllers, which include gas libraries and a gas mixing algorithm. The chamber was maintained under positive pressure to avoid infiltration of ambient air.

Mixing ratios of O₃, CO₂, and water vapor (H₂O) were observed continuously, alternatively sampling the chamber inflow and outflow streams. O₃ was measured by ultraviolet absorption using either a 2B Technologies 202 or 205 Dual Beam Monitor. For experiments prior to July 20, the O₃ instrument (2B Technologies 202) had a time resolution of 0.1 s⁻¹ and an average sample flow rate of 0.609 L min⁻¹ (HelOx), and approximately 0.993 L min⁻¹ (air); for later experiments, the data collection rate improved to 1 s⁻¹ (2B Technologies 205), with a sample flow rate of approximately 1.248 L min⁻¹ (HelOx) and 1.656 L min⁻¹ (air). We measured CO₂ and H₂O by infrared (IR) absorption (LICOR Li7000) at a rate of 2 s⁻¹, requiring a sample flow rate of approximately 0.4 L min⁻¹. Instruments were separately calibrated in air and HelOx atmospheres, with IR absorption measurements being particularly sensitive to band-broadening differences in air and HelOx atmospheres.

Chlorophyll fluorescence was measured using a pulse-amplitude modulation (PAM) fluorometer (Walz PAM-2500). The fiber optic

probe was inserted into the chamber through a PFA union on its top face of the chamber and oriented at approximately 1 cm above the leaf surface at an ~45° angle to the leaf plane such that the saturating light pulse was out of the probe shadow. While effort was taken to standardize the orientation of the fiber optic tip relative to the leaf surface, differences arose both between and during each experiment as the leaf position within the chamber was somewhat variable. The metal surfaces of the fiber optic casing were wrapped in Teflon tape (Swagelok PTFE, MS-STR-4).

Leaf skin temperature was monitored using a Fluke 287 True RMS Multimeter by affixing a Teflon-wrapped thermocouple wire to the leaf underside with polyimide Kapton tape, the area of which (on average 2.192 cm²) was measured and removed from the leaf area calculation.

We treated leaves with either low (15 ppb) and high (75 ppb) O₃ levels under constant CO₂, H₂O, light, and temperature conditions in both air and HelOx. Experiments typically began at 7:00 am with leaf dark adaptation (30 minutes), followed by 1.5 hours of leaf light adaptation, 2 hours of data collection in HelOx, and 2 hours of data collection in air. Experiments were concluded by removing the leaf from the chamber to measure the O₃ flux to chamber surfaces under the O₃ conditions of that day's experiment (15 ppb or 75 ppb), sampling from the pre-chamber air for 15 minutes, followed by the post-chamber air for 15 minutes.

Leaf-level O₃ flux (F_{O₃}). The net chamber O₃ flux (F_{O₃}, nmol m⁻² s⁻¹) is a function of the chamber flow rate (Q, m³ s⁻¹), leaf area (S, cm²), and initial ([O₃]_i, ppb) and outgoing O₃ concentrations ([O₃]_o, ppb) in units nmol m⁻³ (Eq. 2). By convention, flux of O₃ into the leaf has a positive sign.

$$F_{O_3} = \frac{Q}{S} ([O_3]_i - [O_3]_o) \quad (1)$$

The O₃ deposition velocity (V_{O₃}, m s⁻¹) is the absolute value of the slope of the regression line of F_{O₃} versus [O₃]_o.

F_{O₃} precision (s_{F_{O₃}}) was dominated by errors in the O₃ concentration measurement and derived by propagating O₃ precision. Before July 20 sampling rate was 0.1 s⁻¹, and after July 20 sampling rate was 1 s⁻¹. F_{O₃} standard mean error averaged 0.08 nmol m⁻² s⁻¹ before July 20, and 0.03 nmol m⁻² s⁻¹ after July 20. Flow into the chamber was constantly monitored. Standard mean error before July 20 averaged 0.70 L min⁻¹ (HelOx) and 0.30 L min⁻¹ (air), and after July 20 averaged 0.25 L min⁻¹ (HelOx) and 0.34 L min⁻¹ (air).

O₃ uptake on chamber surfaces was characterized by calculating F_{O₃} after removing the plant from the chamber at the end of each experiment. The chamber uptake flux averaged -0.007 nmol m⁻² s⁻¹, and therefore did not contribute significantly to the error in the O₃ flux measurements. On the morning of each experiment, the chamber was flushed with higher than ambient O₃ levels to clean chamber surfaces.

Transpiration (E). The transpiration rate (E, mol m⁻² s⁻¹) was calculated using measurements of the chamber flow rate (Q, mol s⁻¹), leaf surface area (S, m²), and outgoing (w_o, mmol H₂O mol air⁻¹) and initial (w_i, mmol H₂O mol air⁻¹) water vapor mixing ratio (mol H₂O mol air⁻¹), respectively (Eq. S2). Air entering the chamber is saturated, so w_i is 1. All equations were taken from ref (2).

$$E = \frac{Q(w_o - w_i)}{S(1 - w_o)} \quad (2)$$

Errors were propagated from uncertainties defined as 1σ standard mean errors in measured H₂O mixing ratios, and averaged 0.01 mol m⁻² s⁻¹. Uncertainties in Q and S were negligible.

Net CO₂ assimilation rate (A). The rate of net CO₂ assimilation (A, mol m⁻² s⁻¹) was computed from chamber measurements of the flow rate (Q, mol s⁻¹), leaf surface area (S, m²),

outgoing (c_o) and initial (c_i) CO₂ mixing ratios (mol CO₂ mol air⁻¹), and E (Eq. S3).

$$A = \frac{Q(c_i - c_o)}{S} - c_o E \quad (3)$$

Errors were propagated from uncertainties defined as 1s standard mean errors in measured CO₂ mixing ratios, and averaged 0.04 mol m⁻² s⁻¹. Uncertainties in Q and S were comparatively negligible.

Stomatal Conductance. The total water vapor conductance (g_w, mol H₂O m⁻² s⁻¹), which includes both stomatal and boundary layer terms, is equal to Eq. S4. E is the transpiration rate derived in Eq. S2 and W_l and w_o are the water vapor mixing ratios (mmol H₂O mol air⁻¹) within the leaf and leaving the chamber, respectively. The within-leaf mixing ratio (mmol H₂O mol air⁻¹) was calculated from the Eq. 5, where e(T_l) is the water saturation vapor pressure at the leaf temperature (T_l), as measured by a Fluke 287 True-rms Digital Multimeter outfitted with a temperature probe, and P is the atmospheric pressure. All temperatures are in units of °C and all pressures are in units of kPa.

$$g_w = \frac{E(10^3 - 0.5(W_l + w_o))}{(W_l - w_o)} \quad (4)$$

$$W_l = \frac{e(T_l)}{P} 10^3 \quad (5)$$

$$e(T_l) = 0.61365 * \exp\left(\frac{17.502T}{240.97 + T}\right) \quad (6)$$

The stomatal portion of net conductance (g_{s,w}, mol H₂O m⁻² s⁻¹) is described by Eq. S7. k_f was equal to (K² + 1)/(K + 1)², which was 1, where K is the stomatal ratio, an estimate of the ratio of stomatal conductance of one side of the leaf to the other (direct quote, cite LI-6400 manual here). In this case, K is zero because stomata are only present on the bottom side of sweetgum leaves, so k_f = 1. Because the chamber is large relative to the leaf size, and well-mixed such that the leaf flutters visibly in the chamber, we assume boundary layer

resistance is negligible. We approximate the boundary layer conductance as infinite, neglecting the term when calculating stomatal water vapor conductance. A similar assumption was used by Ball (1988) and Mott & Parkhurst (1991).

$$g_{s,w} = \left(\frac{1}{g_w} - \frac{k_f}{g_{b,w}} \right)^{-1} \quad (7)$$

By eliminating the boundary layer conductance term, Eq. S7 can be rewritten such that the total conductance is equivalent to the stomatal portion of net conductance.

$$g_{s,w} = g_w \quad (8)$$

The CO₂ stomatal conductance (g_{s,CO_2} , mol CO₂ m⁻² s⁻¹) follows from Eq. S8 and is given in Eq. S9, where 1.6 is the ratio of the CO₂ and water vapor diffusivity in air/He/O₂, and the boundary layer resistance is once again assumed to be negligible.

$$g_{s,CO_2} = \frac{g_{s,w}}{1.6} \quad (9)$$

Eq. 6 is derived from Buck et al. (1981). All of the equations used above are from the LI-6400 user's manual (Anonymous, 2001).

Results and Discussion

Selecting acceptable data. In total, 13 trials were run under low O₃ conditions, and 14 trials were run under high O₃ conditions. Trials where leaves exhibited irregular behavior or displayed signs of mortality were eliminated. After trials were eliminated according to these standards, there were 9 sets of data for stomata closing under low O₃ conditions, 8 sets for stomata opening under low O₃ conditions, 11 sets for stomata closing under high O₃ conditions, and 8 sets for stomata opening under high O₃ conditions.

Transpiration, Carbon Assimilation, Ozone Flux, and Fluorescence all display oscillatory behavior. Throughout the course of experimentation, transpiration, carbon assimilation, ozone flux signals adjusted to

changes in atmospheric composition as anticipated, increasing or decreasing to a new equilibrium value based on the changes in stomatal aperture. The change was neither direct nor immediate, however. Over the course of each 2-hour period (2 hours for He/O₂, 2 hours for air) the stomatal aperture changed gradually, oscillating as it approached the equilibrium value. These oscillations were strongest as the stomata were closing. Oscillations of transpiration and carbon assimilation are directly proportional to one another and inversely proportional to oscillations of ozone flux. Oscillations were also observed in the fluorescence signal, a phenomenon not previously documented in the literature.

Stomatal Conductance to Water Vapor. By collecting data on a large number of leaves on different days throughout the summer, the data could be analyzed as an ensemble, eliminating inter-leaf variability and variability caused by meteorological conditions. Ensemble data is shown here for stomata closing under low ozone (Fig. 1) and high ozone (Fig. 2) conditions.

From the measured transpiration values, stomatal conductance to water vapor ($g_{s,w}$) was calculated. For stomata closing under high and low O₃ conditions, a strong periodicity was observed in the closure response. Analysis for a difference between closure responses under these two conditions was performed using both a 2-sample t-test and a Wilcoxon rank-sum test. The nature of the oscillations was most consistent in character over the first period, making analysis of associated "short-time" parameters easier. For stomata closing, *p-values* for short-time parameters are given in Table 1. Other parameters, which we call "long-time" parameters, were tested in order to analyze the nature of the closure over its entire duration. Results are given in Table 2. Because this same periodicity was not observed in the stomatal opening response, only some of the parameters characterizing the long-term

behavior of the signal could be analyzed. Test results are given in Table 3. No statistically significant difference between high and low ozone treatment levels was observed at the 95% confidence interval. The data was also tested for confounding effects of meteorological factors. Values of r^2 summarizing these tests are given in Table 4. No effect was observed. For this analysis, stomata closing signals were

analyzed as paradigmatic of the response for the day. Average $g_{s,w}$ was used as an indicator of increased or decreased stomatal activity under different meteorological conditions. Note that temperature and rainfall data were only collected since the beginning of June, so temperature data for June 3, June 4, and June 7 was not averaged over an entire week.

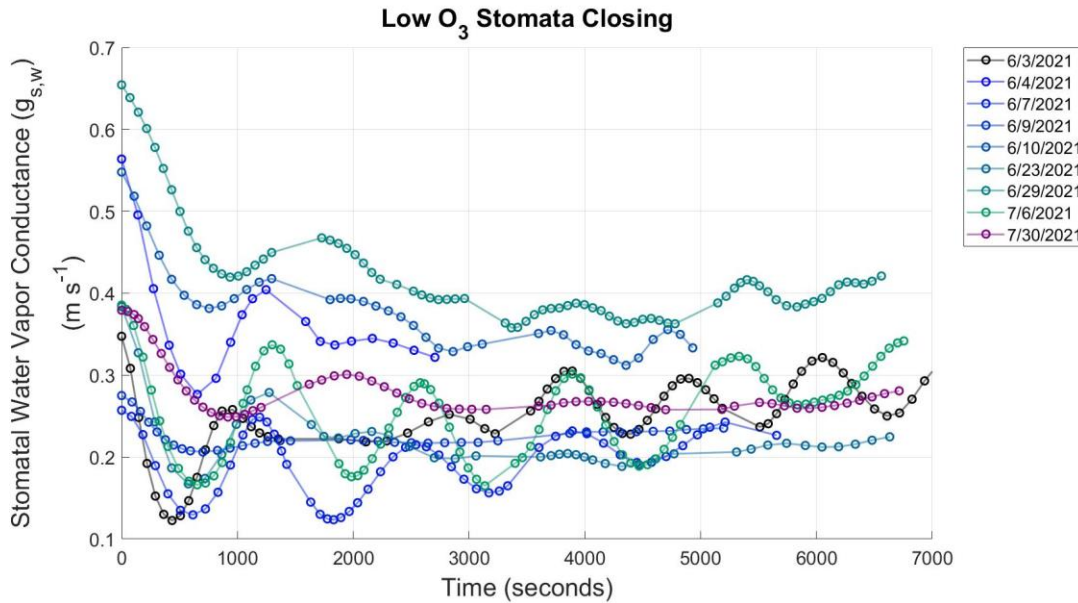


Figure 1. Ensemble of $g_{s,w}$ data for stomata closing under low ozone conditions.

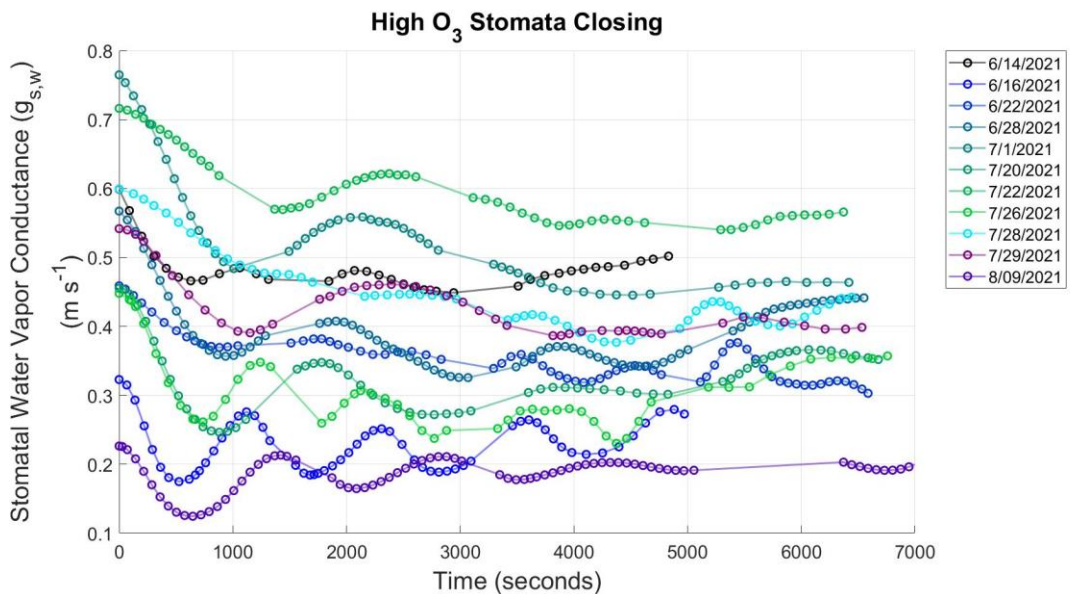


Figure 2. Ensemble of $g_{s,w}$ data for stomata closing under high ozone conditions.

Table 1. Tests for significance for short-time parameters of stomata closing ($g_{s,w}$)

Test	Timing of First Trough	Magnitude of First Trough	Magnitude of First Trough (Normalized)	First Period	First Amplitude	First Amplitude (Normalized)
2-Sample T-Test	0.0755	0.4423	0.0497	0.2089	0.1458	0.1623
Wilcoxon Rank Sum Test	0.1022	0.3619	0.0806	0.2545	0.1965	0.1965

Table 2. Tests for significance for long-time parameters of stomata closing ($g_{s,w}$)

Test	Decrease from Maximum to Equilibrium	Percent Decrease from Maximum to Equilibrium	Decrease from Maximum to Avg. of last 10 points	% Decrease from Maximum to Avg. of Last 10 points	Average Period Length	Average Angular Frequency
2-Sample T-Test	0.9004	0.1010	0.8371	0.5372	0.2183	0.3750
Wilcoxon Rank Sum Test	1.0000	0.0946	0.9394	0.8197	0.4941	0.7304

Table 3. Tests for significance for long-time parameters of stomata opening ($g_{s,w}$)

Test	Increase from Minimum to Equilibrium	% Increase from Minimum to Equilibrium	Increase from Minimum to Avg. of last 10 points	% Increase from Minimum to Avg. of Last 10 points
2-Sample T-Test	0.8596	0.2240	0.4222	0.7181
Wilcoxon Rank Sum Test	0.5737	0.3823	0.4418	0.6454

Table 4. Values of r^2 for the relationship between meteorological variables and $g_{s,w}$

Parameter	r^2 value
Days Since Rain > 0.10 in.	0.155
Temperature on Preceding Day ($^{\circ}$ F)	0.001
Average Temperature During Preceding Week ($^{\circ}$ F)	0.140
Weighted Ozone Concentration on Previous Day (W126, ppm)	0.132
10 Day Weighted Ozone Concentration (W126, ppm)	0.004

Stomatal Conductance to Carbon Dioxide. The same ensemble analysis approach was used to analyze the stomatal conductance to carbon dioxide (g_{s,CO_2}). For stomata closing, p -values for the different tests are given in Tables 6 and 7. For stomata opening, p -values are

given in Table 8. No statistically significant difference between high and low O_3 treatment levels was observed at the 95% confidence interval. As with transpiration there was no confounding effect due to meteorological conditions. Values of r^2 are given in Table 9.

Table 6. Tests for significance for short-time parameters of stomata closing (g_{s,CO_2})

Test	Timing of First Trough	Magnitude of First Trough	Magnitude of First Trough (Normalized)	First Period	First Amplitude	First Amplitude (Normalized)
2-Sample T-Test	0.0755	0.6153	0.0497	0.2089	0.1974	0.1623
Wilcoxon Rank Sum Test	0.1022	0.4941	0.0806	0.2545	0.1965	0.1965

Table 7. Tests for significance for long-time parameters of stomata closing (g_{s,CO_2})

Test	Decrease from Maximum to Equilibrium	Percent Decrease from Maximum to Equilibrium	Decrease from Maximum to Avg. of last 10 points	% Decrease from Maximum to Avg. of Last 10 points	Average Period Length	Average Angular Frequency
2-Sample T-Test	0.9379	0.1010	0.7298	0.5372	0.2183	0.3750
Wilcoxon Rank Sum Test	1.0000	0.0946	0.8792	0.8197	0.4941	0.7304

Table 8. Tests for significance for long-time parameters of stomata opening (g_{s,CO_2})

Test	Increase from Minimum to Equilibrium	% Increase from Minimum to Equilibrium	Increase from Minimum to Avg. of last 10 points	% Increase from Minimum to Avg. of Last 10 points
2-Sample T-Test	0.789	0.2240	0.3887	0.7181
Wilcoxon Rank Sum Test	0.6454	0.3823	0.3823	0.6454

Table 9. Values r^2 for the relationship between meteorological variables and g_{s,CO_2}

Parameter	r^2 value
Days Since Rain > 0.10 in.	0.093
Temperature on Preceding Day (°F)	0.009
Average Temperature During Preceding Week (°F)	0.210
Weighted Ozone Concentration on Previous Day (W126, ppm)	0.183
10 Day Weighted Ozone Concentration (W126, ppm)	8.17E-04

Fluorescence. Two fluorescence parameters were collected by the PAM-2500 sensor. F_m' is the maximum fluorescence level during a treatment. It is induced by a saturating light pulse that temporarily closes all photosystem II (PSII) reaction centers. Non-photochemical quenching causes this value to decrease with respect to F_m . F is the momentary fluorescence yield (F_t) of an illuminated sample shortly before a saturation pulse is applied (Anonymous, 2019). This is steady-state fluorescence. Because F_m' has the clearest oscillatory trends, it was used for this analysis.

The fluorescence signal is in units of relative intensity. Reliable measurements are dependent upon the probe being positioned a consistent distance from and angle to the leaf surface. Steps were taken to make leaf distance and angle as consistent as possible between trials, but turbulent mixing conditions and the leaf wilting within the chamber led to an inevitable change in distance and angle, associated with a gradual decline in signal intensity. The MATLAB ‘detrend’ function

was used to correct for this, leaving behind only the oscillations in F_m' that are due to photosynthetic response of the leaf. Unfortunately, too few of the trials displayed a consistent oscillatory response to test for significant differences between treatment levels.

We are able to compare the detrended data to carbon assimilation data to look for trends. On days when oscillations are strong, they start out closely matched to carbon assimilation data. By the end of the day, the two signals are often out of phase. On days with no oscillations in F_m' , no correlation can be observed. Carbon assimilation and fluorescence values have been shown to correlate with one another when averaged over a long time period. It’s also been documented that elevated O_3 exposure levels can cause these two values to decouple. However, on the short timescales used in this experiment, we cannot necessarily expect that the two signals would be coupled, and so we cannot look for evidence of decoupling. What is instead significant is that oscillations in fluorescence are observed in the first place. We

would expect that the perturbations in stomatal diffusive resistance would impact a stomatally driven parameter like carbon assimilation, but this suggests that the perturbations also impact processes taking place in the photosystem itself. F_m' in particular is the proportion of available photons being put towards fluorescence and heat dissipation rather than photosynthesis. As F_m' increases, there is more fluorescence and less photosynthesis. Stressors can be one reason that a plant would divert photons away from photosynthesis, with the purpose of not introducing more stress to the photosynthetic machinery. While the respiratory behavior of the leaves included in this analysis remained normal throughout the duration of this experiment, it's reasonable to assume that there is some underlying level of stress as a result of having been removed from their host tree. As carbon assimilation decreases and photosynthesis becomes more carbon limited, it is possible that the leaves, likely already stressed, are diverting more photons away from photosynthesis, thus increasing F_m' . This may explain why the signals are out of phase towards the end of each experiment, even though they start off in phase.

There is also no evidence that meteorological conditions have influenced the nature of these oscillations.

Conclusions

Tropospheric O_3 has been documented to reduce carbon assimilation in plants. This study sought to determine the mechanism by which this damage occurs. Stomatal diffusive resistance was alternating a chamber atmosphere between air and He/O_2 under both low and high O_3 conditions, allowing us to manipulate stomatal conductance without confounding effects on O_3 chamber lifetime and plant metabolism. Leaves from ozone-exposed sweetgum trees, *Liquidambar styraciflua*, were tested and O_3 and CO_2 uptake, transpiration, leaf temperature, and chlorophyll fluorescence were monitored. We conclude

that O_3 uptake is stomatally limited and that there is no evidence for an internal rate-limiting resistance. Transpiration, carbon assimilation, and their coupling are not impacted by isolated elevated O_3 exposures of 75 ppb for 2 hours. Stomatal sluggishness and a decoupling between carbon assimilation and photosynthesis, two phenomena reported elsewhere in the literature, were not observed. As changes in stomatal aperture induced fluctuations in carbon assimilation, these same fluctuations were observed in the fluorescence signal, suggesting a closer connection between carbon assimilation and photosynthesis on small timescales than previously realized.

Acknowledgements

We would like to thank the National Science Foundation (NSF, AGS 1837891) for financially supporting this project. We are also grateful for the additional support provided by the Virginia Space Grant Consortium Undergraduate STEM Research Scholarship and the University of Virginia Harrison Undergraduate Research Award to Jacob Bushey.

References

- Anonymous (2001). Using the LI-6400: Portable Photosynthesis System. ed Biogeosciences L-C (Lincoln, Nebraska).
- Anonymous (2019). PAM-2500 Portable Chlorophyll Fluorometer: Handbook of Operation. ed Heinz Walz GmbH (Effeltrich, Germany).
- Ball, J.T. (1988). An Analysis of Stomatal Conductance. (Publication No.) [Doctoral dissertation, Stanford University]. Carnegie Institution for Science.
- Breuninger, C., Meixner, F. X., and Kesselmeier, J. (2013). Field investigations of nitrogen dioxide (NO_2) exchange between plants and the atmosphere. *Atmos. Chem. Phys.*, 13(2), 773–790. <https://doi.org/10.5194/acp-13-773-2013>

- Buck, A.L. (1981). New Equations for Computing Vapor Pressure and Enhancement Factor. *Journal of Applied Meteorology* 20(12):1527-1532.
- Delaria, E.R., et al. (2018). Measurements of NO and NO₂ exchange between the atmosphere and *Quercus agrifolia*. *Atmospheric Chemistry and Physics*, 18(19), 14161-14173. <https://doi.org/10.5194/acp-18-14161-2018>
- Lombardozi, D., et al. (2012). Ozone exposure causes a decoupling of conductance and photosynthesis: implications for the Ball-Berry stomatal conductance model. *Oecologia*, 169(3), 651-659. <https://doi.org/10.1007/200442-011-2242-3>
- Meixner, F. X., Fickinger, T., Marufu, L., Serca, D., Nathaus, F. J., Makina, E., Mukurumbira, L., and Andreae, M. O. (1997). Preliminary results on nitric oxide emission from a southern African savanna ecosystem. *Nutr. Cycl. Agroecosys.*, 48, 123–138.
- Mott, K.A., & Parkhurst, D.F. (1991). Stomatal responses to humidity in air and helox. *Plant, Cell & Environment*, 14(5), 509-515.
- Paoletti, E., & Grulke, N.E. (2010). Ozone exposure and stomatal sluggish in different plant physiognomic classes. *Environmental Pollution*, 158(8), 2664-2671. doi:10.1016/j.envpol.2010.04.024
- Pape, L., Ammann, C., Nyfeler-Brunner, A., Spirig, C., Hens, K., and Meixner, F. X. (2009). An automated dynamic chamber system for surface exchange measurement of non-reactive and reactive trace gases of grassland ecosystems. *Biogeosciences*, 6(3), 405– 429. <https://doi.org/10.5194/bg-6-405-2009>
- Parkhurst, D.F., & Mott, K.A. (1990). Intercellular Diffusion Limits to CO₂ Uptake in Leaves. *Plant Physiology*, 94(3), 1024-1032.
- Torsethaugen, G., et al. (1999). Ozone inhibits guard cell K⁺ channels implicated in stomatal opening. *Proceedings of the National Academy of Sciences of the United States of America*, 96(23), 13577-13582.